An active feedback scheme for low field NMR experiments

Emmanuel Baudin, Kayum Safiullin, Steven W. Morgan, Pierre-Jean Nacher

Preprint - January 2011 *To be published in Journal of Physics: Conference Series*

An active feedback scheme for low field NMR experiments

Emmanuel Baudin[1], Kajum Safiullin[1], Steven W. Morgan[1,2] and Pierre-Jean Nacher[1]

Abstract. In low field nuclear magnetic resonance (NMR) it is desirable to combine proper characteristics of the detection scheme with a good signal to noise ratio. For example, a reduced coupling between the sample and the detection coil is needed for NMR with highly magnetized samples and a large bandwidth is required in magnetic resonance imaging (MRI). We discuss a solution based on a simple active feedback circuit that preserves the signal to noise ratio as opposed to traditional solutions which do not. We give illustrations of its use in experiments on low temperature hyperpolarized liquid ^{3}He-^{4}He mixtures and in hyperpolarized ^{3}He gas MRI.

[1] Laboratoire Kastler Brossel, ENS; CNRS; UPMC; 24 rue Lhomond, F-75005 Paris, France.
[2] Laboratoire Structure et Dynamique par Résonance Magnétique, IRAMIS, CEA, CNRS, UMR 3299 SIS2M, CEA/Saclay, 91191 Gif-sur-Yvette, France.

E-mail: nacher@lkb.ens.fr

1. Introduction

Nuclear magnetic resonance (NMR) detection schemes are usually based on resonators tuned to the Larmor precession frequency f_L which are strongly coupled to the sample (with a large geometrical filling factor). A high quality factor (Q-factor Q) of the resonator provides a Q-fold signal enhancement and contributes to a high signal-to-noise ratio (SNR) of the recordings.

Though achieving a high SNR is desirable, the high Q-factor has the drawback of enhancing the interaction between the sample and the detection coil, leading to (often) unwanted radiation damping: the emf induced by the precessing magnetization drives a rf current in the resonator at precisely the Larmor frequency, and the oscillating magnetic field associated with this current tends to drive the magnetization into its stable orientation along the applied static magnetic field. When the magnetization is close to its stable orientation, radiation damping leads to a reduction of the lifetimes of the observed signals, known since the early days of NMR [1]. Radiation damping can also lead to unstable precession or to maser operation, and additional modifications of NMR precession (frequency shifts due to so-called cavity pulling) result from sample-resonator coupling if the latter is detuned. In this paper we will focus on the control of radiation damping, but cavity pulling can likewise be manipulated.

A high Q-factor also narrows the bandwidth $\Delta f = f_\mathrm{L}/Q$ of the detection circuit and leads to a long characteristic response time Q/f_L for any changing signals. This introduces severe limitations in *low frequency* NMR, where recovery from equipment saturation and ring-down due to rf pulses can prevent the observation of short-lived NMR signals. It also limits the spatial resolution of low frequency magnetic resonance imaging (MRI), for which broadband acquisition of rapidly changing signals in strong imaging gradients is required.

The usual solution to reduce radiation damping consists in decreasing the Q-factor or the filling factor, i.e., degrading the reception properties of the resonator. In doing so, the SNR is unfortunately reduced as well. For MRI applications, Q-spoiling can indeed be used to address the bandwidth limitation issue as well [2], but this also reduces SNR. Another solution to the bandwidth limitation consists in correcting the recorded signal using a numerical filter in post-processing [3, 4]. This compensates for the frequency response characteristics, but strongly degrades SNR at the edges of the resonator bandwidth, and may introduce artifacts in MRI when large corrections are involved. Transiently reducing the Q-factor whenever saturating rf pulses are applied by introducing so-called Q-switches is a widely used method to limit the adverse impact of a high Q-factor on fast recovery, but this only partly alleviates ringdown problems.

Active feedback schemes have been proposed and successfully used to independently address these issues. To our best knowledge, Hoult was the first to use a negative feedback scheme together with a Q-switch device [5] to efficiently reduce recovery time for NMR operating at 5 MHz without loss of SNR. Two feedback schemes [6] have been proposed to strongly reduce current in resonators, hence to suppress radiation damping: The 'Brussels' scheme [7] uses inductive coupling of the suitably amplified signal, in such a way that the feedback emf tends to oppose the emf induced by precessing magnetization. The 'Ecole Polytechnique' scheme [8] uses directional couplers to feed back the suitably amplified signal to the NMR resonator. For MRI applications, the only non-dissipative bandwidth broadening scheme we are aware of is based on the use of over-coupled high-Q NMR coils [9]. It provides adequate bandwidth for operation at several MHz with no SNR penalty.

In this paper we propose an implementation of an active feedback circuit that solves both the coupling and the bandwidth problems at very low frequency, and we report on its efficiency in two applications involving hyperpolarized ^{3}He in NMR and MRI around 2.5 mT. The device relies on the same inductive coupling of the feedback as the 'Brussels' scheme but operates at high impedance and has been used for different purposes. Beyond these examples, the potential uses of such a scheme cover all situations where non-perturbing, accurate low field NMR measurements are performed, e.g., to monitor polarization in gas hyperpolarization systems, in polarized ^{3}He targets or neutron spin filters, and in ^{3}He or ^{129}Xe magnetometry.

2. An active feedback scheme for low frequencies

Figure 1 shows the detection circuit schematic including the active feedback scheme we use for low-frequency (below 100 kHz) NMR signal detection. At such low frequencies, propagation delays in connecting cables are totally negligible and impedance matching with 50 Ω cables is useless. It is actually more convenient to use high-impedance detection tank circuits and preamplifiers having medium to high input impedance and suitably low voltage and current noise. We report results obtained using a Stanford Research Systems 560 preamplifier (voltage noise 4 nV/$\sqrt{\text{Hz}}$, current noise 2 fA/$\sqrt{\text{Hz}}$, input impedance 100 MΩ + 25 pF gain 1-50,000). Impedances of the tank circuits at resonance are 2.5 kΩ and 35 kΩ in our applications, thus the effect of current noise is negligible. Signal recordings are made from the output of this preamplifier. An electronic circuit called a "feedback control box" is used to modify the relative phase and amplitude of the signal fed back into the detection circuit. This control is essential as it determines the reduction factor of the interaction between the sample and the detection coil and ensures the stability of the closed loop circuit.

The feedback control box is built using standard low frequency electronic circuitry. We use a phase shifter [10] to change the phase of the loop signal relative to the output signal without affecting its amplitude. This decoupling between the controls of amplitude and phase allows one to easily realize optimal and reproducible settings. The electronic loop is coupled to the tank circuit using a transformer with a small self-inductance compared to the detection

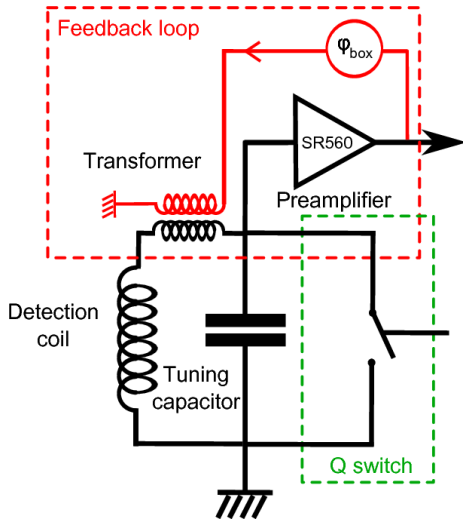

Figure 1. Active feedback schematic. The detection tank circuit, tuned at Larmor frequency f_{L}, is formed by the detection coil in parallel with a capacitor. It includes the secondary winding of a low-inductance transformer used with the feedback control box φ_{box} for adjustable feedback. In the MRI application, an electronic switch (Q-switch) is connected in parallel with the tank circuit. This fast-switching device allows for a strong reduction of the Q-factor as its resistance is of the order of 50 Ω when closed, much lower than the impedance of the tank circuit at resonance (35 kΩ).

coil self inductance (1/100th), thus leaving the resonance frequency of the tank circuit almost undisturbed. The transfer function of the feedback loop mainly determines the spoiling of the Q-factor and may also produce a small shift in the resonance frequency of the detection circuit, depending on the details of the feedback loop. It is convenient to distinguish the Q-factor in the open loop configuration Q, which is the one of the free tank circuit, and the Q-factor of the closed loop circuit Q_{FB}, which is the Q-factor associated with the linewidth of the frequency response of the circuit with the active feedback.

As with any active electronic circuit, the detection circuit stability depends on the choice of the feedback settings. Several features can lead to deviations from the expected behavior. In particular, one has to consider the linear Nyquist stability of the circuit. The use of the feedback control box allows for a fine tuning of the phase necessary to meet the Nyquist stability criterion with high feedback gains. The dynamic range of the feedback scheme is also limited by the non-linearity and saturation of the amplifier used in the loop.

In the next section, we describe two experiments operating at similar frequencies but for which detection circuits have different Q-factors, Johnson noise, and bandwidth: ^{3}He NMR at low temperature and ^{3}He MRI at room temperature. We thus explore two different regimes for the active feedback configuration, but in both experiments Q_{FB} of order $Q/40$ was achieved.

3. Two applications of the low frequency active feedback device

3.1. Reduction of radiation damping in low temperature ^{3}He NMR

Our group performs NMR studies on dense hyperpolarized ^{3}He-^{4}He liquid mixtures (at 1K), in which the distant dipolar field resulting from the large sample magnetization plays the dominant role in the NMR free evolution, provided that radiation damping is avoided [11]. To assess the effect of the interaction between the sample and the coil, we use ^{3}He gas at 4.2 K instead of liquid: with this reduced density, distant dipolar effects have a negligible role in NMR evolution. Hyperpolarized ^{3}He is contained in a 0.44 cm^3 spheroidal cell. NMR is performed using a shielded transmit coil orthogonal to a saddle-shaped detection coil, which is part of a tank circuit resonant at 74 kHz with $Q = 14$. This modest Q-factor results from resistive losses in the cryogenic coaxial cable used between the coil and the tuning capacitor, but in spite of this the thermal (Johnson) noise is small compared to the preamplifier noise. Signal acquisition and rf sequences, which can be quite elaborate on liquid samples [11], are performed using a Tecmag Apollo console.

For the radiation damping studies used here as an illustration of the active feedback detection performance, hyperpolarized ^{3}He gas with polarization up to 20% is used. Following a small

tipping angle rf pulse, an exponentially decreasing signal is observed. Since the intrinsic transverse relaxation time is long (hours), relaxation is due to fast atomic diffusion in the weak field inhomogeneities. In this motional averaging regime, exponential relaxation is expected, with rates depending only on the field map and on the spin diffusion coefficient. However, decay rates which scale with signal amplitudes are observed. This behaviour is characteristic of the radiation damping effect for magnetization orientation near the stable direction [1, 6].

Figure 2 shows typical free induction decay signals for experiments in which different configurations of the detection scheme have been used. For the standard detection coil (a) for which the Q-factor is Q=14, the signal damping rate is 0.22 s^{-1}. When a suitable resistor

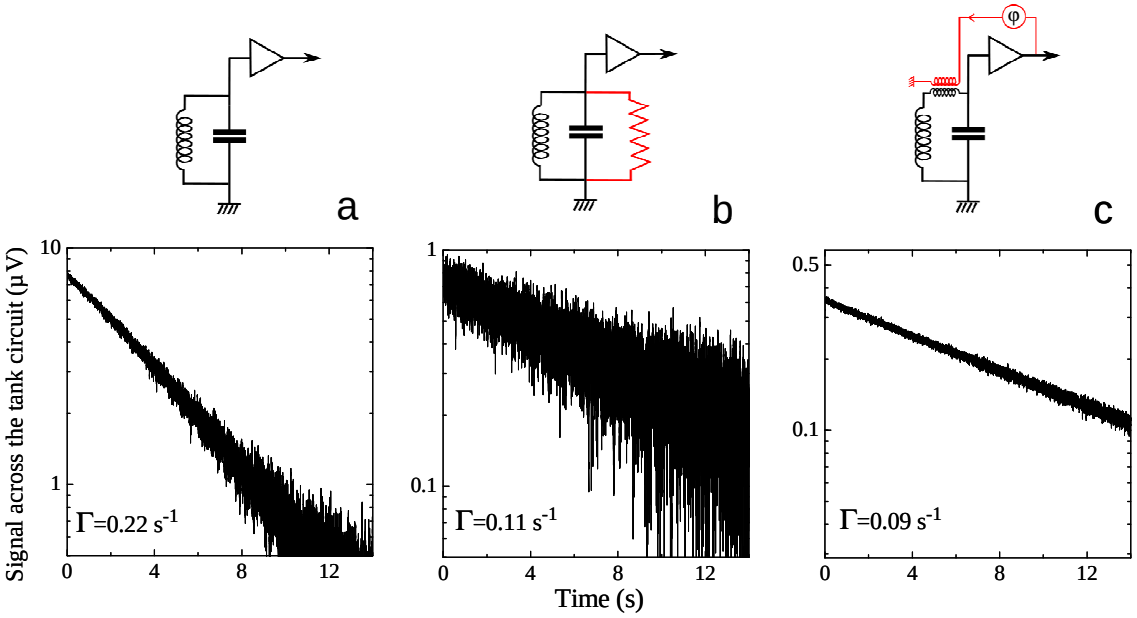

Figure 2. Signals recordings in semilog scale for three circuit configurations: standard tank circuit (a), Q-spoiled circuit (b), and tank circuit with feedback (c). These recordings have been obtained using hyperpolarized ^{3}He gas at 4.2 K (polarization ∼14%, pressure ∼1 torr) after a 9° tipping rf pulse. The vertical scales take into account the electronic gains and refer to voltage amplitudes across the capacitor.

is used in parallel with the capacitor to spoil the Q-factor to Q_S=1.4 (b), the signal damping rate is reduced to 0.11 s^{-1}, but the signal is attenuated (÷10) and the SNR is significantly reduced. When active feedback is used (c), a radiation damping-free signal is obtained with a damping rate of 0.09 s^{-1} and a signal to noise ratio similar to that of case (a) in spite of a smaller signal amplitude (÷22 in this case). The additional damping rate introduced by coupling to the unspoiled detection circuit is found to be $\Gamma_{RD} \sim 0.13$ s^{-1}. This is consistent with expectations relying on tip angle calibrations for pulsed NMR performed using the detection coil for both rf transmit and pick-up.

The striking feature of the signals obtained using active feedback is that in spite of the strong reduction of the voltage across the detection coil (Figure 2c), the SNR is fully preserved: no passive dissipation is introduced, and the amplifier noise is reduced by the feedback loop with the same factor as the detected signal. This detection scheme is now systematically used instead of the initial Q-spoiled scheme [11] to suppress radiation damping in our NMR studies of hyperpolarized liquid helium. It will also be used to enhance the coupling between the coil and the sample magnetization in a well-controlled way. This will allow further studies of the

combined effects of distant dipolar fields and radiation damping that can lead to yet another kind of spin turbulence [12].

3.2. Fast, broadband detection in ^{3}He MRI

We use a home-built low frequency MRI setup designed for small animals [13] that operates at f_L=85 kHz (corresponding to a static magnetic field of 2.7 mT). Combining Litz wire in detection coils with low-loss capacitors, Q-factors typically range from 100 to 200 depending on coil size. The required detection bandwidth corresponding to the frequency span due to the imaging gradient over the image's field of view is about 10 kHz. It could be simply achieved by spoiling the Q-factor of the detection circuit down to $Q_S \sim$10 with a resistor. But at such a low frequency in this MRI setup, the Johnson noise of the room-temperature unspoiled circuit is of the same order of magnitude or larger than the preamplifier noise, and both are the significant sources of total noise on the output. Thus, a simple spoiling of the circuit leads to a significant increase of dissipation as well as to a reduction of the signal output, both effects leading to a degradation of the SNR. The active feedback circuit added to the high-Q tank circuit allows us to dramatically increase the detection bandwidth without affecting the SNR. A comparison of the main computed properties of a simply spoiled circuit and a circuit with active feedback for parameters corresponding to the experimental conditions is shown in Fig. 3.

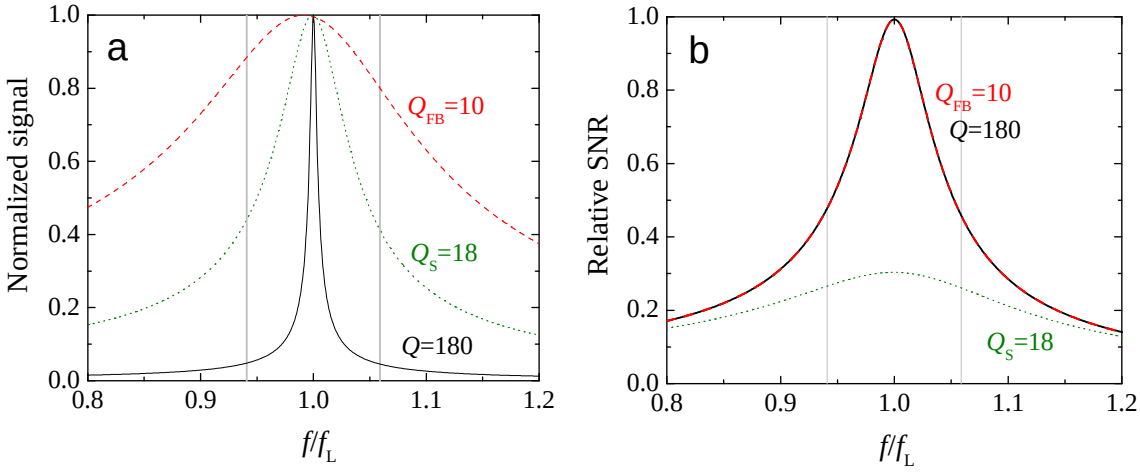

Figure 3. Computed relative amplitudes (a) and SNR (b) of the detection circuit expected for the three circuit configurations illustrated in Fig. 2. **a:** Both Q spoiling and feedback broaden the tank circuit bandwidth. For each curve, the amplitude is normalized to the value at resonance. The vertical grey lines represent the limits of the region of interest for MRI. **b:** The corresponding SNRs are normalized to the SNR of the unspoiled circuit at resonance. Feedback does not affect the SNR (overlaid upper curves) but Q spoiling decreases SNR over the MRI bandwidth by a factor of 2 to 3.

Figure 3a shows that, over the frequency range of interest, the active feedback circuit (with Q=180, Q_{FB}=10) has a flat enough frequency response and only requires small amplitude corrections, whereas the Q-spoiled and unspoiled circuits would require significant and very large corrections, respectively. Active feedback does not change the SNR (Fig. 3b): signal and noise are identically scaled by the feedback at all frequencies. The SNR of the Q-spoiled circuit is substantially degraded due to increased dissipation and to an increasing noise contribution from the preamplifier. The feedback scheme thus combines the high SNR of the high-Q circuit and the suitably flat amplitude response of a Q-spoiled circuit.

Another important advantage of using active feedback is the faster recovery of the detection circuit. Simple experimental examples of ringdown after rf-pulse saturation of a detection system with Q=100 are shown in Fig. 4. Using active feedback decreases the 'dead-time' and

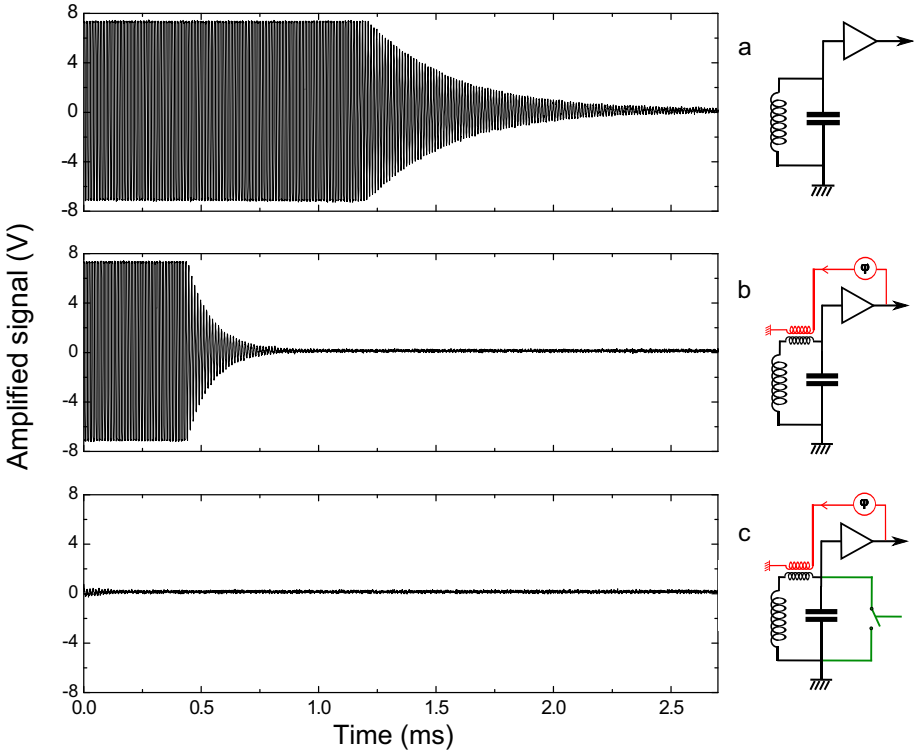

Figure 4. Experimental ringdowns recorded just after the end of a typical NMR tipping pulse. Recovery from saturation of the detection system is shown for different configurations of the detection circuit. **a**: A standard Q=100 tank circuit was used. **b**: The active feedback circuit is used, providing a reduced Q-factor Q_{FB}=25. **c**: Both active feedback and Q-switch were used. The duration of the ringdown is then sufficiently short to make acquisitions as soon as 100 μs after the end of the tipping pulse.

using an additional Q-switch (strong spoiling of the Q-factor of the coil during the rf-pulse) almost removes it completely. In the test experiment of Fig. 4c, a small parasitic signal remains for 150 μs, probably because of the Q-switch energy injected into the tank circuit during the switch opening, so data acquisition would be affected and must be blanked only during this time. This allows us to use fast pulse sequences, with acquisition periods as short as to 2 ms. The improvement is made possible thanks to the availability of low charge injection CMOS analog switch circuits which introduce less than 1 pC into the tank circuit when switching, thus minimizing disturbance of the NMR acquisition.

Figure 5 is an illustration of a successful utilization of active feedback in a low field MRI experiment. The active feedback has been used to obtain an image of gas in a sealed glass cell (1.8 cm $\times$ 12 cm) containing 400 mbar of ^{3}He polarized to a fraction of a percent[1] using a Fast Low Angle SHot (FLASH) sequence. Short acquisition times had to be used to avoid strong signal attenuation in highly diffusive gas, so echoes were recorded for 4 ms with a 10 kHz sampling rate. The tank circuit used for this image consisted of a pair of rectangular coils

[1] At high pressure, laser polarization is quite inefficient which explains this very small polarization. Still, total magnetization is higher than in typical low-pressure cells, and slower gas diffusion makes MRI possible

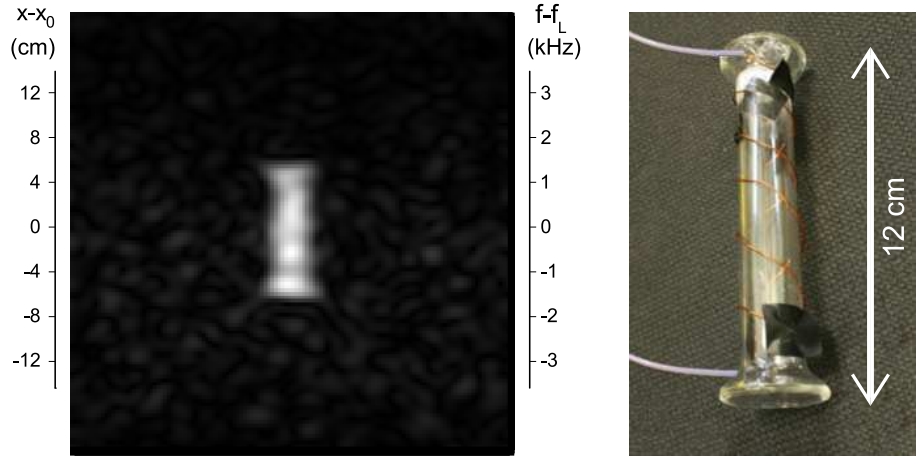

Figure 5. MRI image (left) obtained on a sealed glass cell (pictured on right) using hyperpolarized ^{3}He (polarization $\sim$ 0.5%). A FLASH imaging sequence was used (32 $\times$ 38 points, 12° tip angle, echo time 2.5 ms, acquisition time 4 ms).

(5 cm×15 cm, 4 cm apart, 36 turns each, Litz wire consisting of 25 strands of 0.1 mm) and a low-loss C0G capacitor (2.2 nF). Its high Q-factor (Q=180) would normally yield a grossly insufficient bandwidth (f_{L}/Q=0.5 kHz) but the use of feedback extended the detection bandwidth to about 6 kHz. As a result, the noise pattern is quite uniform over the image, a feature made possible by the use of the active feedback instead of bandwidth correction as was done in references [3, 4]. Additionally, the scheme lessens ring-down effects that plague low field NMR. This could be useful for solid state NMR at low frequencies.

Acknowledgments

This research program is supported in part by the Agence Nationale de la Recherche (ANR DIPOL grant) and by the European Commission (PHeLINet Marie Curie Research and Training Network grant).

References

[1] Bloembergen N and Pound R V 1954 *Phys. Rev.* **95** 8–12
[2] Tsai L L, Mair R W, Rosen M S, Patz S and Walsworth R L 2008 *J. Magn. Reson.* **193** 274–285
[3] Bidinosti C P, Choukeife J, Nacher P J and Tastevin G 2003 *J. Magn. Reson.* **162** 122 – 132
[4] Ruset I C, Tsai L L, Mair R W, Patz S, Hrovat M I, Rosen M S, Muradian I, Ng J, Topulos G P, Butler J P, Walsworth R L and Hersman F W 2006 *Concepts Magn. Reson. B* **29B** 210–221 ISSN 1552-5031
[5] Hoult D I 1979 *Rev. Sci. Instrum.* **50** 193–200 URL `http://link.aip.org/link/?RSI/50/193/1`
[6] Jeener J 2002 *Encyclopedia of Nuclear Magnetic Resonance, Volume 9: Advances in NMR* (John Wiley & Sons)
[7] Broekaert P and Jeener J 1995 *J. Magn. Reson. A* **113** 60–64
[8] Louis-Joseph A, Abergel D and Lallemand J Y 1995 *J. Biomol. NMR* **5** 212–216
[9] Raad A and Darrasse L 1992 *Magnetic Resonance Imaging* **10** 55 – 65 ISSN 0730-725X URL `http://www.sciencedirect.com/science/article/B6T9D-4BX2CCT-8/2/82914e7fb2ebf60c653330b5800967fb`
[10] Horowitz P and Hill W 1989 *The Art of Electronics* (Cambridge University Press)
[11] Hayden M E, Baudin E, Tastevin G and Nacher P J 2007 *Phys. Rev. Lett.* **99** 137602
[12] Lin Y Y, Lisitza N, Ahn S and Warren W 2000 *Science* **290** 118–121
[13] Nacher P J, Pelissier M and Tastevin G 2007 *Proc. Intl. Soc. Mag. Reson. Med. 15* p 3290 ISSN 1545-1428